European Journal of Pharmaceutics and Biopharmaceutics 78 (2011) 36–48

Contents lists available at ScienceDirect

European Journal of Pharmaceutics and Biopharmaceutics

journal homepage: www.elsevier.com/locate/ejpb

Research paper

Examination of drug release and distribution from drug-eluting stents with a vessel-simulating flow-through cell

Anne Seidlitz [a,*], Stefan Nagel [a], Beatrice Semmling [a], Niels Grabow [b], Heiner Martin [b], Volkmar Senz [b], Claus Harder [c], Katrin Sternberg [b], Klaus-Peter Schmitz [b], Heyo K. Kroemer [d], Werner Weitschies [a]

[a] Institute of Pharmacy, Biopharmaceutics and Pharmaceutical Technology, EMA University of Greifswald, Greifswald, Germany
[b] Institute for Biomedical Engineering, University of Rostock, Rostock, Germany
[c] Biotronik SE & Co. KG, Erlangen, Germany
[d] Institute of Pharmacology, Research Center of Pharmacology and Experimental Therapeutics, EMA University of Greifswald, Greifswald, Germany

ARTICLE INFO

Article history:
Received 14 September 2010
Accepted in revised form 9 December 2010
Available online 21 December 2010

Keywords:
Drug-eluting stent
In vitro dissolution
Vessel-simulating flow-through cell
Finite element modelling
Spatial distribution
Vessel-simulating compartment

ABSTRACT

The recently introduced vessel-simulating flow-through cell offers new possibilities to examine the release from drug-eluting stents in vitro. In comparison with standard dissolution methods, the additional compartment allows for the examination of distribution processes and creates dissolution conditions which simulate the physiological situation at the site of implantation. It was shown previously that these conditions have a distinct influence on the release rate from the stent coating. In this work, different preparation techniques were developed to examine the spatial distribution within the compartment simulating the vessel wall. These methods allowed for the examination of diffusion depth and the distribution resulting in the innermost layer of the compartment simulating the vessel wall. Furthermore, the in vitro release and distribution examined experimentally were modelled mathematically using finite element (FE) methods to gain further insight into the release and distribution behaviour. The FE modelling employing the experimentally determined diffusion coefficients yielded a good general description of the experimental data. The results of the modelling also provided important indications that inhomogeneous coating layer thicknesses around the strut may result from the coating process which influence release and distribution behaviour.

Taken together, the vessel-simulating flow-through cell in combination with FE modelling represents a unique method to analyse drug release and distribution from drug-eluting stents in vitro with particular opportunities regarding the examination of spatial distributions within the vessel-simulating compartment.

1. Introduction

Since their first approval in 2002, millions of drug-eluting stents (DES) have successfully been implanted. Up to date, however, many questions regarding in vivo drug release and the desired release profiles remain unanswered [1]. Whereas first in vivo studies suggested that long periods of release are absolutely necessary to induce the desired pharmacological effect [2,3], findings of Scheller et al. [4] indicate that very short contact times between the vessel wall and a Paclitaxel-eluting balloon may be suitable to deliver sufficient amounts of drug. Besides the remaining uncertainties regarding the desired release profiles, there is only limited data available on the actual in vivo release behaviour of DES. In vivo release studies in humans are limited by the fact that drug plasma levels if above the limit of quantification are not necessarily representative of the concentrations within the vessel wall tissue which is the site of action for the released antiproliferative agents [5]. The explanatory value of animal models, in which removal of the respective tissue and direct analysis is feasible, is also limited due to different healing and restenosis rates and the fact that the arteries are typically non-arteriosclerotic [6]. Furthermore, studies by Hwang et al. [7] suggest that release from DES may lead to large concentration gradients in the vessel wall. Therefore, mean tissue concentrations may be misleading.

In order to examine the release and distribution from DES independent of animal models, standardised dissolution testing is performed using compendial apparatuses such as the reciprocating holder and the flow-through cell and non-compendial methods [8]. These methods may provide insight into the release from the stent coatings under standardised conditions but cannot be used to evaluate distribution processes since they lack a compartment simulating the vessel wall. In order to overcome this limitation, we

* Corresponding author. Address: Institute of Pharmacy, Biopharmaceutics and Pharmaceutical Technology, University of Greifswald, Friedrich-Ludwig-Jahn-Strasse 17, 17487 Greifswald, Germany. Tel.: +49 3834 864898; fax: +49 3834 864886.
E-mail address: anne.seidlitz@uni-greifswald.de (A. Seidlitz).

0939-6411/$ - see front matter © 2010 Elsevier B.V. All rights reserved.
doi:10.1016/j.ejpb.2010.12.021

recently developed a vessel-simulating flow-through cell [9]. This method is based on the compendial flow-through cell. The adapted test system, however, includes a hydrogel compartment representing the vessel wall and emulates the geometry of stent placement within a blood vessel. The DES is implanted into an opening in the hydrogel hollow cylinder which is then perfused by perfusion liquid at a flow rate that corresponds to the blood flow velocity in coronary arteries. In this three-compartmental setup, the analysis of distribution processes under the applied conditions becomes feasible. Experiments using this setup also showed that the applied embedding and flow conditions markedly changed the release rate from the coatings compared to compendial dissolution testing [9].

It was the objective of this work to demonstrate different possibilities to examine distribution patterns experimentally and theoretically. Based on the previously described dissolution experiments [9], the release and distribution in the vessel-simulating flow-through cell from stents coated with the fluorescent model substances fluorescein sodium und triamterene were mathematically modelled and compared to experimental results. Fluorescein sodium was chosen as a hydrophilic compound (freely soluble in water (0.1-1 g/ml) [10], log $P = -1.52$ [11]), whereas triamterene served as a model hydrophobic drug (solubility in water 28 μg/ml [12], log $P = 1.25$ [13]). Release and distribution in the vessel-simulating flow-through cell were simulated as diffusion processes in a two-dimensional finite element model. Alternatively, two experimental methods to visualise spatial distribution within the hydrogel compartment were developed to evaluate stents coated with the model substance rhodamine B (very soluble in water (>1 g/ml) [10], log $P = 2.30$ [14]).

2. Materials and methods

2.1. Materials

Sodium alginate was purchased from Fagron GmbH & Co. KG (Barsbüttel, Germany). Eudragit® RL and RS were provided by Evonik Röhm GmbH (Darmstadt, Germany). All further reagents were of analytical grade.

2.2. Stent coating

Bare metal stents (BMS, type: PRO-Kinetic, nominal diameter 3.5 mm), generously provided by Biotronik GmbH (Berlin, Germany), were coated by dipping as previously described [9]. The resulting coatings contained 20–25% fluorescent model substance (calculated in percentage of total solid content of coating fluid) embedded in a ammonio methacrylate copolymer type A and B blend (Eudragit® RL/Eudragit® RS, ratio 3:7). In order to evaluate coating thickness, two stents were exemplarily embedded in epoxy resin and cross-sections were prepared (Histo Saw DDM-P 216, Medim, Giessen, Germany). After grinding and polishing with aluminium oxide suspension, these microsections were examined by confocal microscopy (Confocal Scanning Laser Microscope LEXT OLS 3000, Olympus, Hamburg, Germany).

2.3. Vessel-simulating flow-through cell

The compendial standard flow-though cell for tablets with a diameter $d = 22.6$ mm was modified (Fig. 1) as previously described elsewhere [9]. In brief, an acrylic glass disc with a hole in the centre ($d = 3$ mm) was inserted into the cell onto which a calcium alginate gel compartment with a cylindrical opening in the centre ($d = 3$ mm) was placed. DES were expanded into the opening by means of a balloon catheter and a catheter pump (6 atm, 15 s). 250 ml of perfusion liquid phosphate buffered saline pH 7.4 (PBS) according to Ph. Eur. were circulated through the vessel-simulating flow-through cell in a closed system setup at a flow rate of 35 ml/min, which corresponds to the blood flow velocity in coronaries [15]. Perfusion liquid and flow-through cell were placed in a water bath and maintained at 37 °C during the intended incubation period.

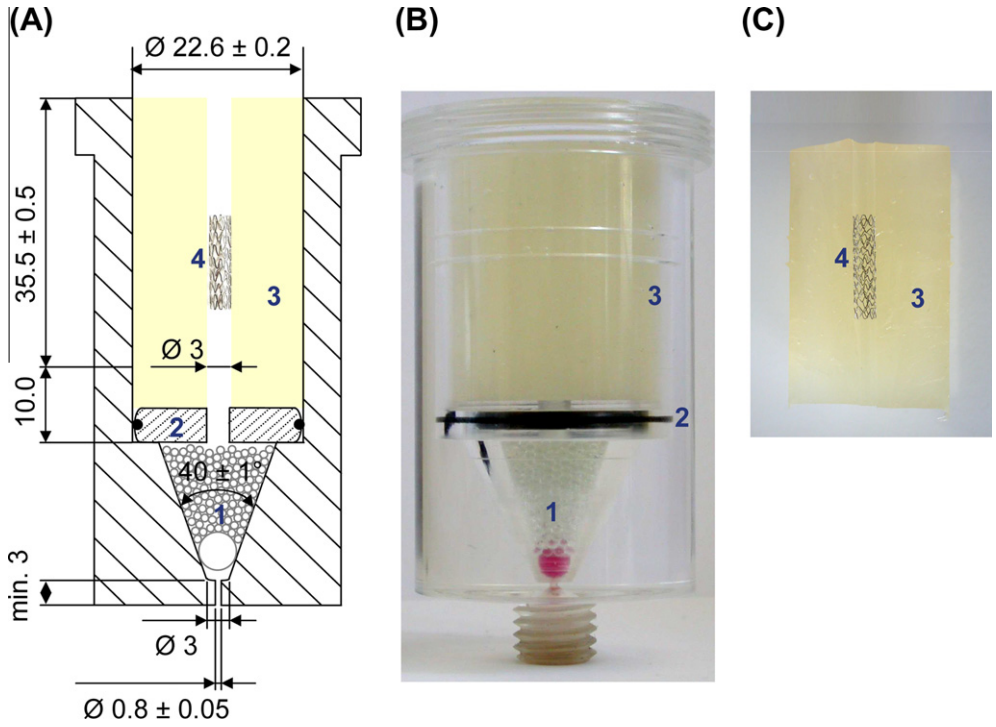

Fig. 1. Schematic and photograph of the vessel-simulating flow-through cell (A and B) and longitudinal section of the hydrogel cylinder with implanted stent (C). (1) Glass beads, (2) acrylic glass disc, (3) hydrogel and (4) expanded stent.

2.4. Spatial distribution within the vessel-simulating compartment

Two different experimental setups were developed for the analysis of the spatial distribution within the hydrogel after incubation with rhodamine B coated stents. Fluorescence imaging of cross-sections of the gel cylinder were performed for a qualitative detection of the fluorescent probe concentrations. For this purpose, the DES was removed after the intended incubation period. The hydrogel cylinder was divided into appropriately sized sections of approximately 10 mm length and placed on cork discs. The aperture was filled with Tissue-Tek OTC Compound (DiaTec Labortechnik GmbH, Hallstadt, Germany). Subsequently, shock freezing by liquid nitrogen cooled petroleum ether at −80 °C was performed and microtome cryosections with a width of 20 μm were prepared (Microm HM 550, Microm International, Walldorf, Germany). The obtained sections were dried immediately and inspected in a fluorescence microscope (Axiovert 200, Carl Zeiss MicroImaging GmbH, Jena, Germany, λ_{ex} 546 nm/$\lambda_{em} \geqslant$ 590 nm, microscopic imaging via AxioCam HrC, Carl Zeiss MicroImaging GmbH, Jena, Germany).

For imaging of spatial distribution patterns in hydrogel regions in direct contact with the struts and the perfusion liquid, alginate films were prepared with a doctor blade (width 500 μm) using a diffusion controlled gelling mechanism. The alginate solution (3% (m/m) in purified water) was topped with a solution of calcium chloride 6% (m/m) in purified water, left to set for 10 min and fixed centrally in the vessel-simulating flow-through cell. For this purpose, the films were coiled around the stainless steel rod which serves as a placeholder during hydrogel solidification [9]. After setting of the surrounding hydrogel, the rod was removed leaving an aperture in the hydrogel surrounded by the coiled alginate film. The DES was then implanted directly into the film and perfused. At the end of the intended incubation period, the surrounding hydrogel was removed. The film was uncoiled, transferred to a specimen slide and imaged via fluorescence microscopy (see above).

2.5. Quantitative analysis of release and distribution

In our theoretical model, release as well as distribution processes in the vessel-simulating flow-through cell are described by diffusion. The diffusion equation

$$\frac{\partial c}{\partial t} = D \cdot \frac{\partial^2 c}{\partial x^2}, \tag{1}$$

in this case written in its one-dimensional form, correlates variations of the concentration c in time and space via the diffusion coefficient D. General solutions can be obtained for simple geometries [16]. The desorption from an infinite plane sheet of thickness l into stirred media with constant concentration via one surface is given by the equation

$$\frac{m_t}{m_0} = \sum_{n=0}^{\infty} \frac{8}{(2n+1)^2 \cdot \pi^2} \cdot \exp\left(-\frac{D \cdot (2n+1)^2 \cdot \pi^2 \cdot t}{4l^2}\right) \tag{2}$$

in which m_0 denotes the initial total mass contained in the sheet and m_t the respective mass at time t [16].

For modelling of dissolution experiments in the vessel-simulating flow-through cell, two-dimensional diffusion problems in two compartments described by the equations

$$\frac{\partial c_i}{\partial t} = -\nabla \cdot J_i, \quad J_i = -D_i \nabla c_i, \quad i = c, h \tag{3}$$

were considered. ∇ denotes the gradient (∇c_i) or the divergence ($\nabla \cdot J_i$) operator. The subscripts c and h refer to coating and hydrogel, respectively. Solely one of Eq. (3) is valid for the geometries 1 (equation for $i = c$) and 2 (equation for $i = h$) as described below. The flux J_i is determined by the concentration gradient and the diffusion coefficient D_i valid for the diffusion of the model substance in the compartment i.

The following geometries were considered (see also Fig. 2):

Geometry 1: Diffusion out of a homogeneously loaded coating layer of thickness l around a quadratic strut (edge length 100 μm) into infinite perfusion liquid, boundary conditions $J = 0$ for the inner surface of the coating (no flux into the metal), $c = 0$ for the outer surface (release into stirred perfusion liquid under sink conditions).
Geometry 2: Diffusion out of a homogeneously loaded hollow cylinder ($d_{outside}$ = 22.6 mm, d_{inside} = 3 mm) into infinite perfusion liquid passing through the aperture in the cylinder, boundary conditions $J = 0$ for the outer surface of the hollow cylinder (contact with the apparatus wall, no flux), $c = 0$ for the inner surface of the hollow cylinder (release into stirred perfusion liquid under sink conditions).
Geometry 3: Diffusion out of a homogeneously loaded coating layer of thickness l around a quadratic strut (edge length 100 μm) into a segment of a hollow cylinder ($d_{outside}$ = 22.6 mm, d_{inside} = 3 mm, segment angle α calculated according to volume ratio of stent coating and hydrogel), boundary conditions $J = 0$ for the inner surface of the coating (no flux into the metal) and the outer surface of the hollow cylinder (contact with the apparatus wall, no flux), $J_h = J_c$ for the continuity of mass flux at the interface between hydrogel and stent coating. Two different sets of boundary conditions were considered at the luminal border as follows: geometry 3a: $J = 0$ for the luminal side of the coating and the inner surface of the hollow cylinder (no perfusion liquid present, no contact with a diffusible compartment); geometry 3b: $c = 0$ for the luminal side of the coating and the inner surface of the hollow cylinder (infinite stirred perfusion liquid passing through the lumen).

For numerical calculation, we used the commercial finite element (FE) software ABAQUS (Dassault Systèmes Simulia Corp., Providence, USA, version 6.7-3). Model size was reduced by considering geometrical symmetries and the introduction of boundary conditions. The flux across symmetry planes was set to $J = 0$. The two-dimensional models were constructed using a suitable mesh of 8-node biquadratic elements. The meshes were generated using ABAQUS routines and contain about 400 (geometry 1), 800 (geometry 2) and 7300 (geometry 3a and 3b) elements. Cell density was greatest near interfaces where high concentration gradients are expected. A typical mesh is illustrated in Fig. 3. Accuracy of calculation was tested for simple geometries (planes, cylinders) and some combinations of flux and concentration boundaries for which analytical results are available [16]. Coating layer thickness l was calculated from the coating layer mass, the stent surface according to the manufacturer specification and the density of the coating. The FE modelling was performed with concentrations normalised by the solubility s_i in the compartment i according to the equation

$$\phi_i = c_i / s_i \tag{4}$$

The normalised concentrations, ϕ_i, are continuous at the border of different materials and determine the partitioning of diffusing substances when equilibrium is achieved. The solubility of the model substances in the hydrogel was approximated based on the solubility in water. The solubility in the polymer layer was assumed to equal the amount of drug substance incorporated. In order to determine under which conditions FE modelling is mandatory for the description of our experiments, the release from an infinite plane sheet was calculated according to Eq. (2) and compared to the modelled release from coating layers on quadratic struts of differing thicknesses. The diffusion coefficients of the

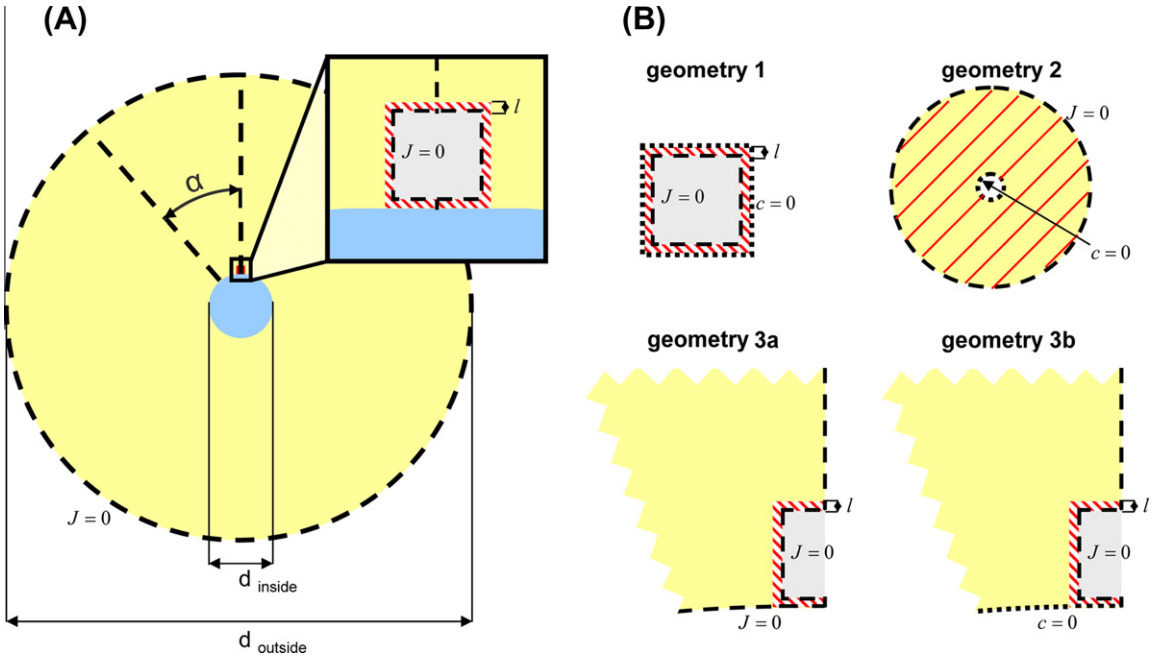

Fig. 2. Schematics of the conditions in the vessel-simulating flow-through cell (A, cross-section, inlay magnifying the position of a stent strut) and the two-dimensional geometries considered for FE calculations (B, geometry 3a and 3b depicting magnified portion of A). Geometry 1: release from a drug loaded coating of a stent strut into infinite stirred media represented by boundary condition $c = 0$ (no hydrogel present); geometry 2: release from a drug loaded hydrogel hollow cylinder into infinite stirred media represented by boundary condition $c = 0$ (no stent strut present); geometry 3a: release from a drug loaded coating of a stent strut into a hydrogel hollow cylinder (no perfusion liquid, represented by boundary condition $J = 0$); geometry 3b: release from a drug loaded coating of a stent strut into a hydrogel hollow cylinder and into infinite stirred media passing through the lumen represented by boundary condition $c = 0$. Stent strut with coating of thickness l around the metal core (grey), hydrogel (yellow) with $d_{outside}$ = 22.6 mm, d_{inside} = 3 mm, drug containing compartment hatched in red, perfusion liquid blue, segment angle α calculated according to volume ratio of stent coating and hydrogel, dashed lines denotes boundary condition flux $J = 0$ (symmetry axes or end of diffusible compartment), dotted line marks boundary condition $c = 0$ (release into stirred perfusion liquid under sink conditions).

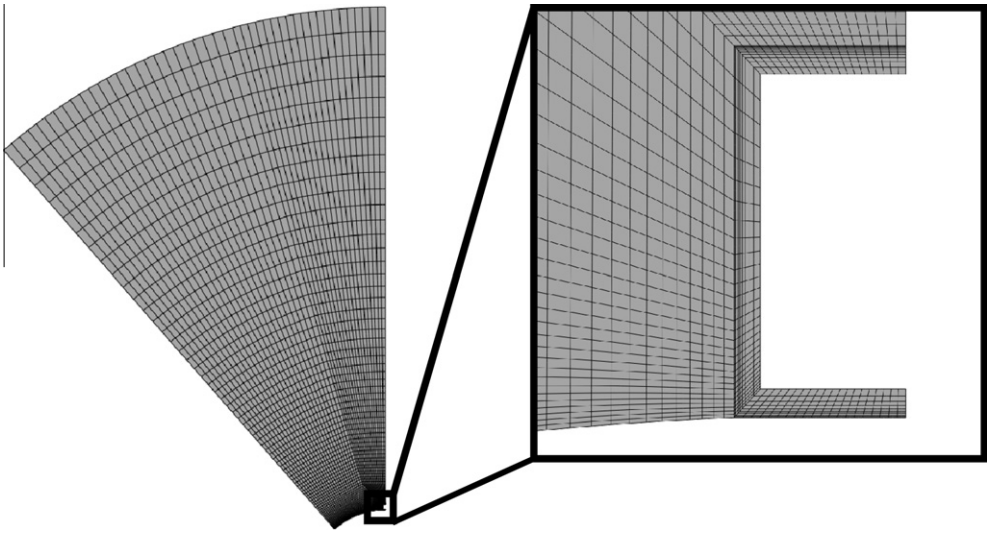

Fig. 3. Schematic of two-dimensional element mesh used for FE calculations of diffusion processes in the vessel-simulating flow-through cell (geometry 3a and 3b), inlay magnifying the stent coating (metal core of strut not modelled) and the adjacent hydrogel region.

model substances in the coating layer as well as in the hydrogel compartment were fitted according to the results of the mathematical modelling and the experiments for geometry 1 and 2 (see below). The determined diffusion coefficients were evaluated by calculating the expected release in geometry 3a and comparing it to experimental data. Finally, the full three-compartmental model (geometry 3b) was calculated and compared to experimental results.

For a detailed characterisation of drug release and distribution processes, experiments were performed under two-compartment conditions (geometry 1, 2 and 3a) and in the complete three-compartmental setup (geometry 3b).

The release from the stent coating into stirred perfusion liquid under sink conditions (geometry 1) was investigated using the compendial standard tablet flow-through cell (USP 4, flow rate 35 ml/min). DES were expanded, placed on top of the glass beads, and the cell was perfused by the perfusion liquid PBS. At the end of the intended perfusion period, the DES was removed from the cell and incubated at least twice in fresh PBS for 24 h each until no further elution from the coating was detectable. The fluorescence

intensity of 200 μl samples of the perfusion liquid, which were drawn from the reservoir during the perfusion at predetermined time points, and the stent incubation buffer was determined using a fluorescence reader (Fluroskan II, Labsystems, Helsinki, Finland, fluorescein sodium: λ_{ex} 485 nm/λ_{em} 538 nm, triamterene: λ_{ex} 355 nm/λ_{em} 460 nm). All measurements were performed in duplicate, and concentration calibration was performed with every experiment. Reduction of perfusion liquid volume due to sampling and evaporation was taken into account in the calculation of model drug content of the perfusion liquid.

The kinetics of distribution in the hydrogel was examined with an experimental setup in which the model substance was homogeneously incorporated in the hydrogel hollow cylinder in the vessel-simulating flow-through cell (geometry 2). For this purpose, the model substances were dissolved in purified water, and these solutions were used for gel preparation instead of purified water. Concentrations of 6.8 μg fluorescein sodium per gram hydrogel and 4.4 μg triamterene per gram hydrogel, respectively, resulted in the loaded hydrogel. The hydrogel hollow cylinder was perfused in the vessel-simulating flow-through cell with 250 ml PBS at a flow rate of 35 ml/min, and the amount released into the perfusion liquid was determined via fluorescence assay as described above.

The transport of model substance from the stent coating into the gel was characterised separately in a third type of two-compartment experiment under omission of the perfusion liquid. After hydrogel preparation, the DES was implanted into the opening in the hydrogel and incubated for predetermined periods of time without perfusion liquid. During incubation at 37 °C, the vessel-simulating flow-through cell was tightly closed. Water loss was not observed. The experiment was terminated after incubation periods ranging from 5 min to 8 h for fluorescein sodium and 5 min to 26 h for triamterene, respectively. Subsequently, the model substance content in the hydrogel and the amount remaining in the stent coating were determined. For this purpose, the DES was removed from the hydrogel and the model substance content of the coating was determined as described above. The hydrogel samples were liquefied by the addition of tenfold concentrated phosphate buffer pH 7.4 according to USP and subsequent stirring. The fluorescence intensity of samples of the stent incubation buffer and the dissolved hydrogel was determined as described above. In the case of the liquefied hydrogel samples, a liquefied blank sample doted with respective model substance concentrations was used for calibration.

The analysis of model substance release from the coating and distribution between the compartments of the vessel-simulating flow-through cell employing fluorescein sodium and triamterene coated stents has been described previously [9]. In brief, the dissolution experiments were terminated after differing incubation periods and model substance content in the perfusion liquid, hydrogel and the amount remaining in the stent coating were determined as described above.

The release and distribution data are presented in percentage of the sum of the amount detected in the respective compartments at the end of the experiment for each geometry (overall detected amount). All amounts were plotted over the square root of time as commonly done for diffusion problems.

3. Results

3.1. Spatial distribution within the vessel-simulating compartment

Fluorescence images of cross-sections of the gel cylinder after incubation with rhodamine B loaded stents are shown in Fig. 4. Without perfusion liquid, a discrete diffusion zone around the lumen was detectable after 5 min incubation time. After 240 min, the whole hydrogel slide showed uniform fluorescence. Under flow-through conditions, the diffusion zone obtained after 5 min was smaller and of lower intensity compared to the hydrogel cylinder incubated without perfusion liquid. At 240 min, only a faint colouration of the hydrogel was detectable. This decrease in fluorescence intensity was obviously due to diffusive washout by the perfusion liquid. Inhomogeneities within the detected diffusion zones, which might have been conceived as a result of direct contact with the stent struts opposed to regions without contact, were not detected.

The images of alginate films allow for the detection of spatial concentration patterns in hydrogel regions adjacent to the lumen and the stent. A collage overview of a film in the fluorescence microscope is shown in Fig. 5A. During the expansion and incubation, the struts are pressed tightly into the alginate film, and the imprints of the struts can be detected after stent removal. Colour intensities of these fluorescence images are influenced by height structure effects, causing the imprints of the struts to be visible as dark lines and the transition zones to appear brightly coloured.

One minute after DES implantation (no perfusion liquid present), an inhomogeneous distribution was detected (Fig. 5B), in which areas close to strut imprints were more lucid. After 5 min (Fig. 5C), a uniform distribution of the fluorescent probe was apparent in the film. Obviously, diffusion in the hydrogel took place quickly, so that the concentration gradients detectable in the hydrogel after 1 min were no longer visible after 5 min of incubation.

The film experiments were also performed under flow conditions with perfusion times of 5 min (Fig. 6A) and 240 min (Fig. 6B). In the film sample which was incubated for 5 min, an intense homogeneously distributed colouration of the film was detectable. Similar to the images obtained from cross-sections after 240 min, only a very faint colouration was visible except for some highlights in the hydrogel regions which had direct contact with strut bends. This decrease in fluorescence intensity can also be attributed to redistribution processes, during which the model substance was transported into other regions of the hydrogel and into the perfusion liquid.

3.2. Quantitative analysis of release and distribution

Prior to the FE modelling of drug release and distribution as diffusion processes in the vessel-simulating flow-through cell setup, the respective diffusion coefficients had to be determined. First, the diffusion from an infinite plane sheet was compared to the diffusive release from stent coatings around quadratic struts (edge length 100 μm) of differing coating layer thicknesses l (geometry 1). The results (Fig. 7) were normalised so that release from the infinite sheet is represented by a single curve independent of coating layer thickness and diffusion coefficient. Deviations of the release of differing stent coatings from this curve are therefore not due to the absolute layer thickness but to effects caused by the different geometry of the coating layer compared to a plane sheet. For the strut edge length of 100 μm, a coating layer thickness l = 10 μm only resulted in a very slight increase in release rate compared to the release from an infinite plane sheet. However, the deviations increased with increasing coating layer thickness. Therefore, the diffusive release from a coating around a quadratic strut can be described by the analytic expression (Eq. (2)), if the coating thickness is small compared to the strut edge length. This condition is valid for the coatings considered in our experiments with a layer thickness in the range of 2 μm and a strut edge length of 100 μm. Therefore, the results of the analytical expression (Eq. (2)) were used to model the release from the stent coating into stirred media under sink conditions. However, for the release from coatings of large layer thickness compared to the strut edge length

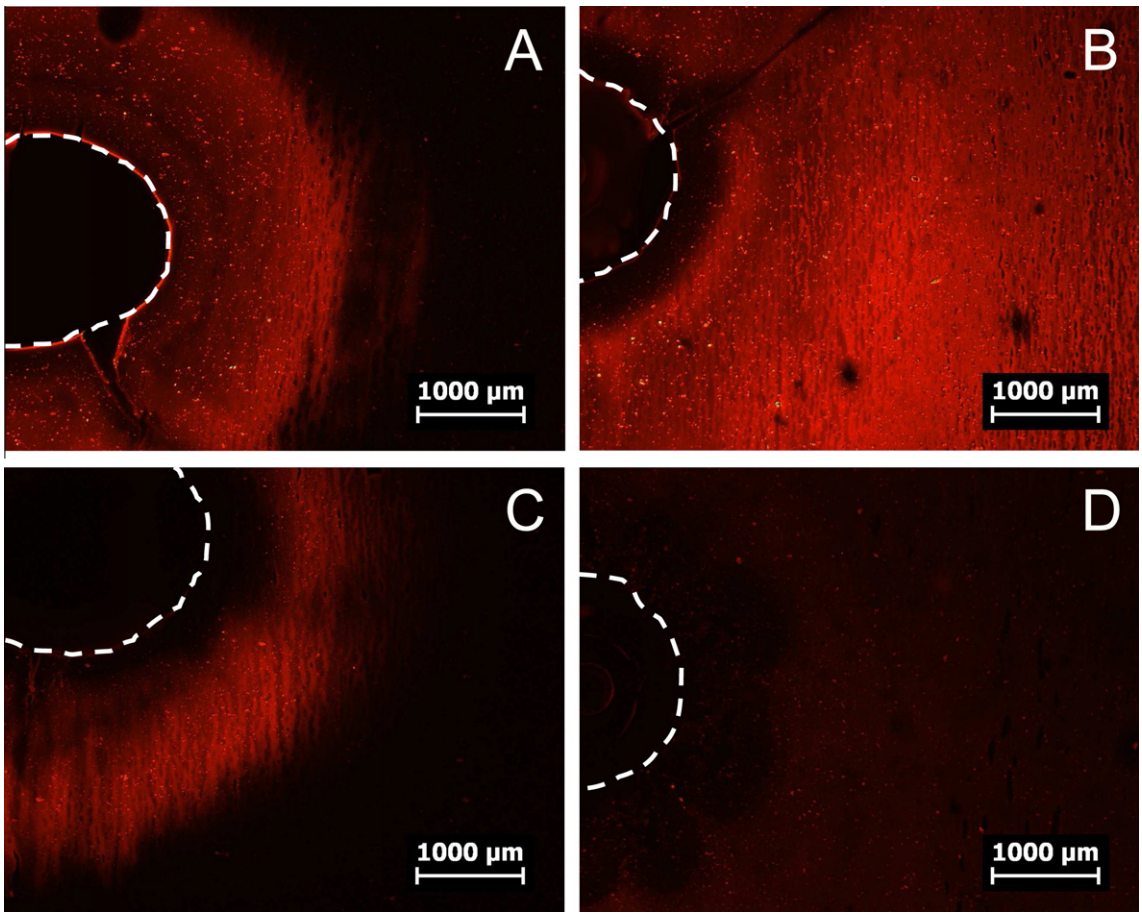

Fig. 4. Fluorescence images of the spatial distribution of rhodamine B in hydrogel cross-sections (width 20 µm) from the vessel-simulating flow-through cell. Incubation without perfusion liquid (A and B) or under perfusion (C and D) for incubation times of 5 min (A and C) or 240 min (B and D). Border between the hydrogel and the opening in which the stents were implanted is indicated by dashed line.

other methods, such as FE modelling, have to be employed, since the deviations from the results of the analytical expression increase with layer thickness, as shown for 40 µm and 80 µm layers (Fig. 7).

In Fig. 8, the experimentally determined release of fluorescein sodium and triamterene from stents into stirred perfusion liquid (geometry 1) is plotted together with desorption lines from plane sheets with the same thickness and various diffusion coefficients. Based on this data, the diffusion coefficients were set to $D_c = 1 \times 10^{-8}$ mm^2/s for fluorescein sodium and $D_c = 2 \times 10^{-10}$ mm^2/s for triamterene.

The experimental release from the hydrogel hollow cylinder initially loaded with model substance into the perfusion liquid is compared to the results of FE calculations for geometry 2 with various diffusion coefficients in Fig. 9.

The diffusion of fluorescein sodium and triamterene in the hydrogel can be described by the same coefficient $D_h = 5 \times 10^{-4}$ mm^2/s. The diffusion coefficients, measures and solubilities for the parameterisation of the release kinetics of the coatings are summarised in Table 1.

The results of the two-compartmental experiment using geometry 3a and the respective FE modelling employing the determined diffusion coefficients are shown in Fig. 10. Every experimental data point represents a separate diffusion experiment with subsequent liquefaction of the hydrogel. In the case of fluorescein sodium, a first period of fast transport from the coating into the hydrogel with a release of approximately 80% was followed by a second period of much slower release. The release of triamterene into the hydrogel cylinder took place at a much slower rate. Applying the diffusion parameters as determined in the former experiments, the FE modelling can describe the biphasic release characteristics of fluorescein sodium as well as the slow transport of triamterene into the hydrogel compartment. In our theoretical model, the period of slower release of fluorescein sodium starts when the coating area which is in direct contact with the gel compartment is nearly exhausted. The transport of the substance remaining in coating areas with no direct contact with the hydrogel (luminal side of the strut) is much slower since the drug has to diffuse through the coating polymer with its low diffusion coefficient towards the polymer regions with hydrogel contact. The same effect was also modelled for triamterene, but at a much later point in time which is not visible in the period of time depicted in Fig. 10.

Results for the FE modelling of the full three compartment system (geometry 3b) as well as the corresponding experimental results are shown in Fig. 11. For fluorescein sodium, the experiments yielded an initially very high fraction of 27% of the overall detected amount of fluorescein sodium in the hydrogel after only 5 min (0.083 h), but the content decreased during further perfusion, obviously due to redistribution into the perfusion liquid. In spite of almost complete depletion of the stent coating after 0.5 h, the model substance fraction detected in the perfusion liquid further increased due to the redistribution processes and amounted to 89% after 8 h. The release from triamterene-eluting stents took place at a much slower rate. After 24 h of perfusion, 6% of total triamterene remained in the stent coating. In the plot over the square root of time, the triamterene content of the stent

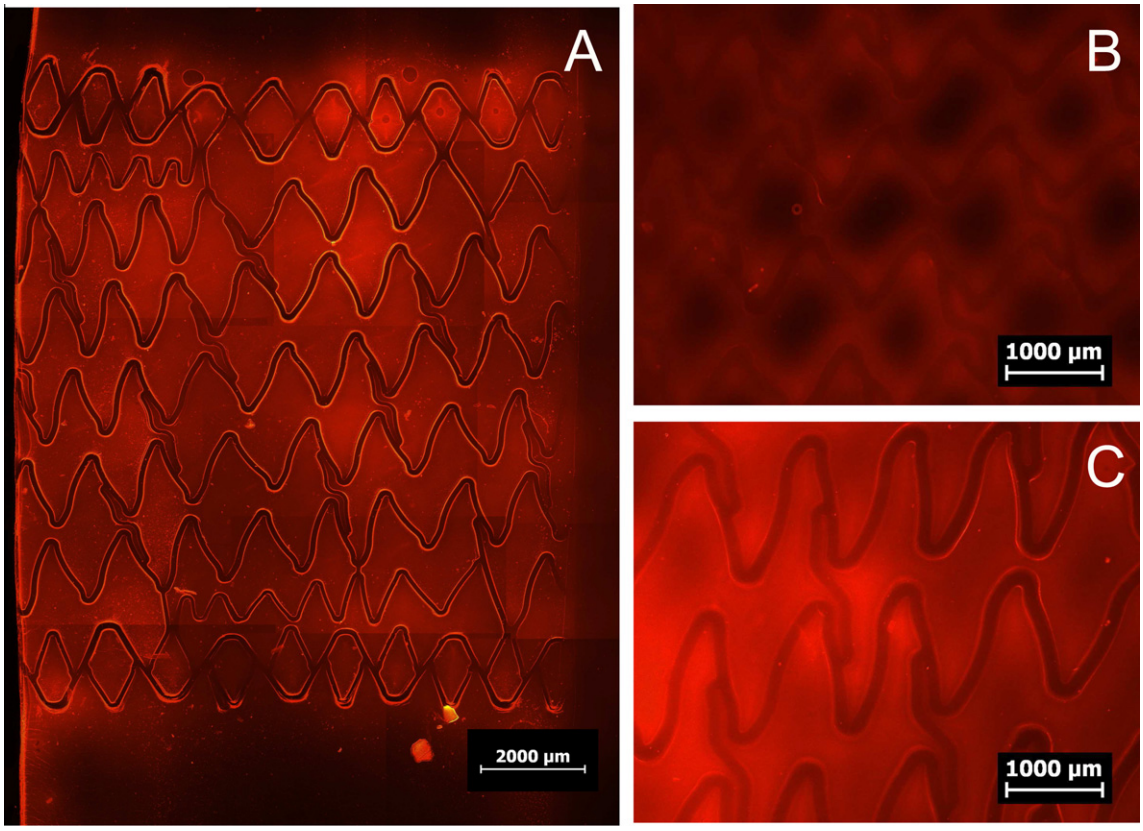

Fig. 5. Fluorescence images of spatial distribution of rhodamine B in alginate films (width 500 µm) fixed in the vessel-simulating flow-through cell at the border between hydrogel and luminal opening. (A) Collage overview of a film sample, (B and C) films incubated with rhodamine B stents for 1 min (B) or 5 min (C) without perfusion liquid.

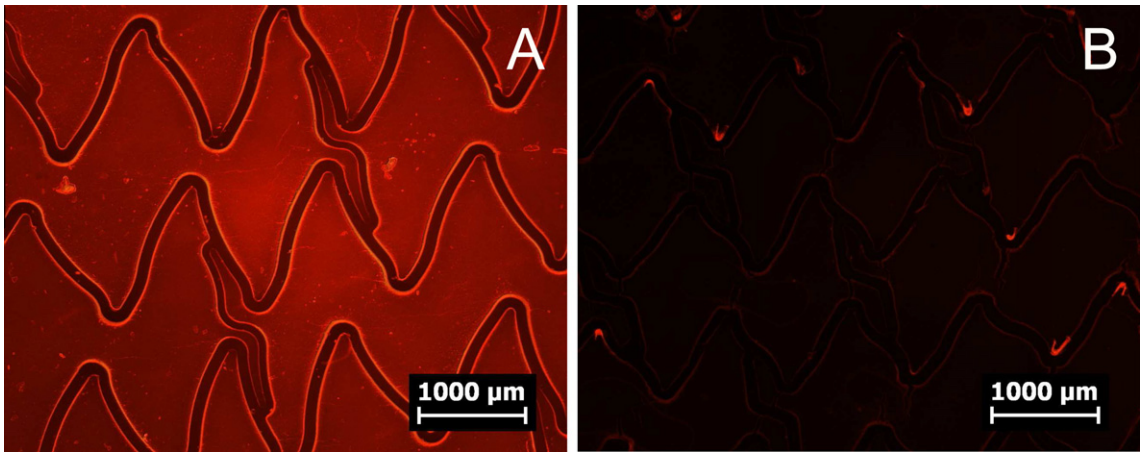

Fig. 6. Fluorescence images of spatial distribution of rhodamine B in alginate films (width 500 µm) fixed in the vessel-simulating flow-through cell at the border between hydrogel and luminal opening. Incubation under perfusion for 5 min (A) or 240 min (B).

coating shows an almost linear decrease. A small peak in hydrogel content was detected after 0.5 h followed by a slight decrease leading to an equilibrium fraction of the total triamterene in the hydrogel during the rest of the experiment. The triamterene fraction detected in the perfusion liquid steadily increased and reached 87% after 24 h. The general distribution behaviour of the two substances was well described by the FE modelling including the release from the coating into the perfusion liquid with temporary accumulation in the gel compartment in the case of fluorescein sodium. However, a quantitative identity was not achieved. For both model substances, the release from the coating was slightly faster in the mathematical model and the fraction detected in the perfusion liquid increased faster and reached a higher endpoint compared to experimental results. Also, the model compound fraction modelled for the hydrogel was lower than experimentally determined for fluorescein sodium as well as triamterene. In the case of triamterene, the drug fraction in the hydrogel slowly increased reaching a maximum after 6 h and then slowly declined again opposed to the early, however small, maximum observed in the experiments after 0.5 h.

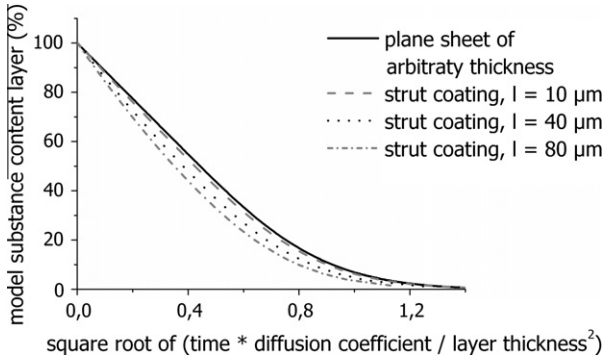

Fig. 7. Normalised desorption from an infinite plane sheet and strut coatings of various thickness into stirred media under sink conditions. Continuous line representing analytical results (plane sheet calculated according to Eq. (2)) and broken lines representing numerical results (strut coating of coating thickness l = 10, 40 or 80 µm, strut edge length 100 µm).

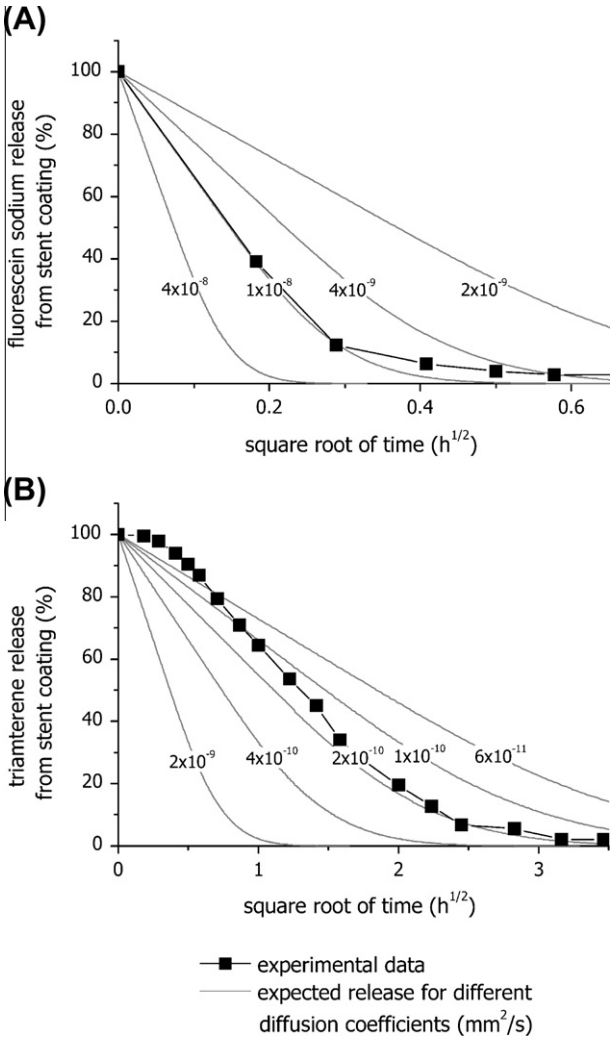

Fig. 8. Normalised release of fluorescein sodium (A) and triamterene (B) from stent coatings in the compendial flow-through cell (geometry 1). Experimental data (squares, n = 6, means) and desorption from an infinite plane sheet into stirred perfusion liquid under sink conditions (lines, analytical results for coating thickness l = 2 µm and different diffusion coefficients as indicated on the graph).

To further adjust the results of the FE modelling to the experimental results and improve the predictability of the mathematical modelling, the influence of an asymmetric coating around the four sides of the strut was investigated in a modified FE model for triamterene. As worst case scenarios in terms of coating homogeneity, a strut without coating on the luminal side and a strut with coating only on the abluminal side were considered. The coating on the remaining sides was assumed to be homogeneously distributed. Based on the calculated coating volume and the reduced coated area, the coating thicknesses were recalculated. To ensure release kinetics into stirred perfusion liquid fitting the experimental data (Fig. 8B), the diffusion coefficient D_c' in the stent coating was rescaled according to the relation

$$D_c' = D_c \cdot (l'/l)^2, \quad (5)$$

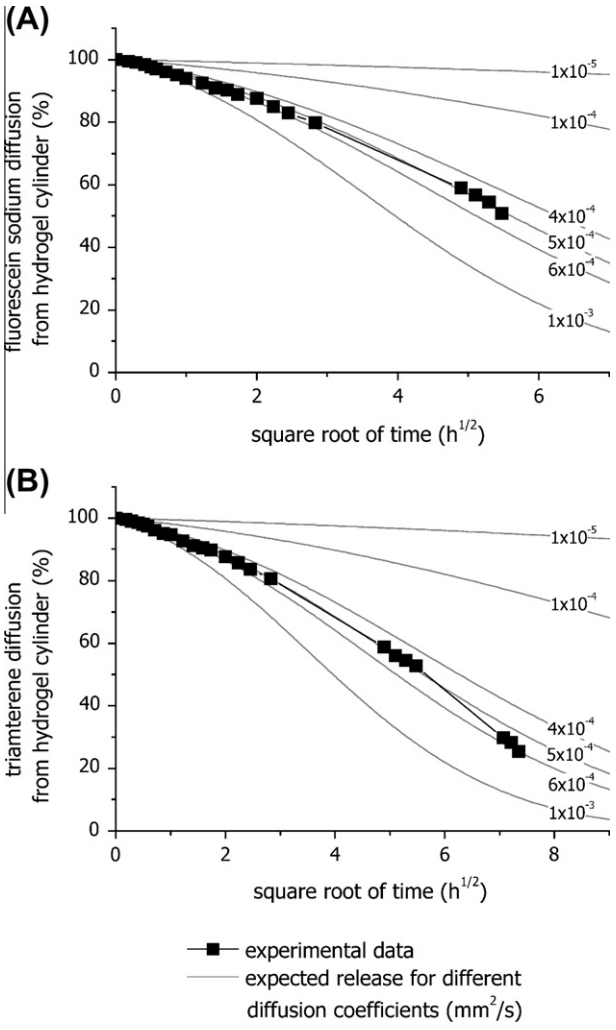

Fig. 9. Normalised diffusion of fluorescein sodium (A) and triamterene (B) from the hydrogel compartment into the perfusion liquid (geometry 2). Experimental data (squares, n = 2, means) and FE calculations of diffusion out of a hollow cylinder ($d_{outside}$ = 22.6 mm, d_{inside} = 3 mm) into stirred perfusion liquid passing through the luminal aperture (lines, for different diffusion coefficients as indicated on the graph).

Table 1
Parameters for the FE modelling of diffusion of fluorescein sodium and triamterene from coated stents in the vessel-simulating flow-through cell.

	Fluorescein sodium	Triamterene
Strut edge length (BMS)	100 µm	100 µm
Mean coating thickness, l	2 µm	2 µm
Solubility in coating, s_c	0.3 g/ml	0.3 g/ml
Solubility in hydrogel, s_h	0.3 g/ml	3×10^{-5} g/ml
Diffusion coefficient in coating, D_c	1×10^{-8} mm²/s	2×10^{-10} mm²/s
Diffusion coefficient in hydrogel, D_h	5×10^{-4} mm²/s	5×10^{-4} mm²/s

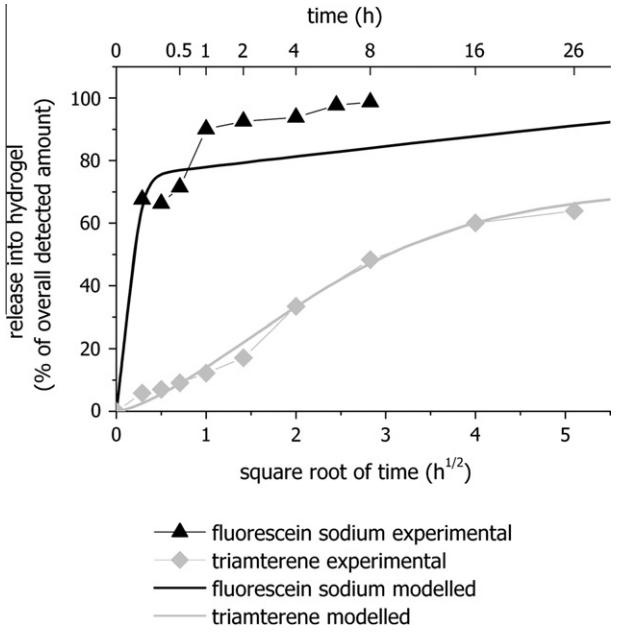

Fig. 10. Normalised amount of model substance released into the hydrogel in the vessel-simulating flow-through cell without perfusion (geometry 3a), experimental data for fluorescein sodium and triamterene (symbols, $n = 3$ for each data point, means) and FE calculations (lines) according to the model parameters listed in Table 1.

in which D_c and l are the parameters originally fitted to the experimental data (Table 1) and l' is the modified coating thickness. For the strut with coatings on the abluminal and lateral sides $l' = 2.7$ μm and $D_c' = 2.9 \times 10^{-10}$ mm^2/s resulted, whereas $l' = 8.2$ μm and $D_c' = 26 \times 10^{-10}$ mm^2/s were calculated for the strut with coating on the abluminal side only. The results of the FE calculations for triamterene-eluting stents using these coating parameters are given in Fig. 12.

The release from a strut with a three-side coating of the abluminal and lateral sides, whose luminal side is not coated, only slightly differed from the FE model with a homogeneous four-side coat. The release rate from the stent coating was however slowed down as intended. A noticeable slower release into the perfusion liquid is obtained for the model in which only the abluminal side of the strut is coated. In this case, the release rate was, however, slower than detected experimentally. A maximum initial accumulation of about 10% of the triamterene in the hydrogel compartment could not be described even with these modifications. But the fraction detected in the perfusion liquid and the distribution at the end of the experiment modelled for the abluminal coating are in good accordance with the experimental data.

In order to examine whether asymmetric coatings may have influenced the experimental release, coating thickness was measured in microscopic images of cross-sections of two stents. An image of a single strut of a microsection is depicted in Fig. 13. Coating thickness data are presented as mean values for the luminal, lateral and abluminal stent side in Table 2. A mean coating thickness of 4.6 μm was measured on the abluminal side opposed to 2.6 μm on the luminal side of a fluorescein sodium coated stent. On a triamterene coated stent, a mean abluminal coating thickness of 5.4 μm was detected whereas the mean coating thickness amounted to 2.7 μm on the luminal side.

4. Discussion

DES are highly specialised medical devices designed to prevent in-stent restenosis by delivering drugs locally to the vessel wall.

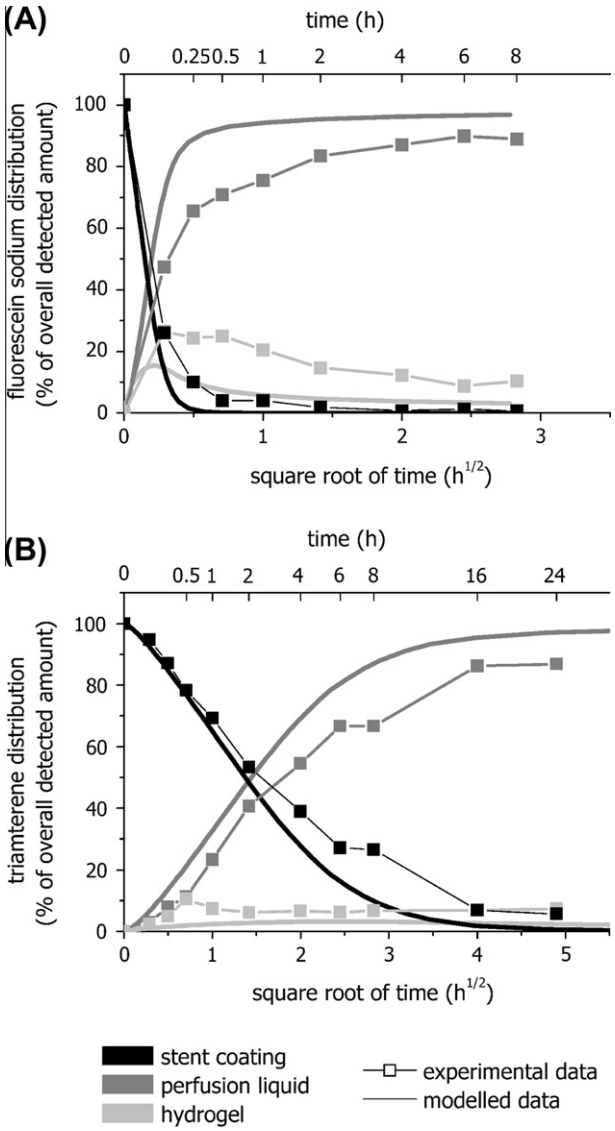

Fig. 11. Normalised amount of the model substances fluorescein sodium (A) and triamterene (B) in the compartments perfusion liquid, hydrogel and stent coating over square root of time (geometry 3b). Experimental data vessel-simulating flow-through cell (squares, $n = 3$ for each data point, means) and FE calculations (lines) according to the model parameters listed in Table 1.

Due to their inherent delivery procedure, they are, however, in direct contact with not only the intended acceptor compartment but also with the flowing blood. Compared to the vessel wall, blood represents a very large and well stirred compartment which is responsible for the reduction of the amount of drug available for penetration into the vessel wall. Therefore, not only the release from the coating but also the distribution of the released substances between the blood and the vessel wall is of major importance for the concentration at the site of action.

The vessel-simulating flow-through cell was developed to address the questions arising from this particular situation in a three-compartmental setup (stent coating, perfusion liquid simulating the blood and hydrogel representing the vessel wall). The developed setup also takes the placement of the DES (abluminal side in direct contact with the solid compartment and directional perfusion liquid flow through the centre) as well as the blood flow velocity into account. As shown previously, these embedding and flow conditions have a distinct influence on the release rate from the stent coating [9].

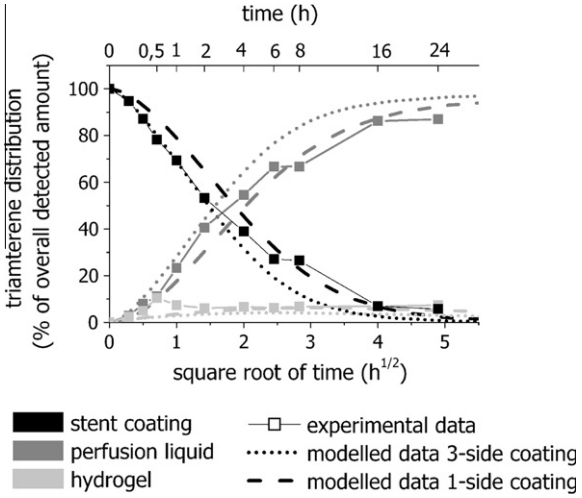

Fig. 12. Normalised amount of triamterene in the compartments perfusion liquid, hydrogel and stent coating over square root of time (geometry 3b) under adaptation of the FE calculations based on the assumption of asymmetrical coatings. Experimental data vessel-simulating flow-through cell (squares, $n = 3$ for each data point, means) and FE calculations for asymmetrical coatings (lines) according to the model parameters listed in Table 1 with adapted diffusion coefficient D_c' and coating layer thickness l' (3-side coating: coating on the abluminal and lateral sides, $l' = 2.7$ μm and $D_c' = 2.9 \times 10^{-10}$ mm²/s, 1-side coating: coating on the abluminal side only, $l' = 8.2$ μm and $D_c' = 26 \times 10^{-10}$ mm²/s).

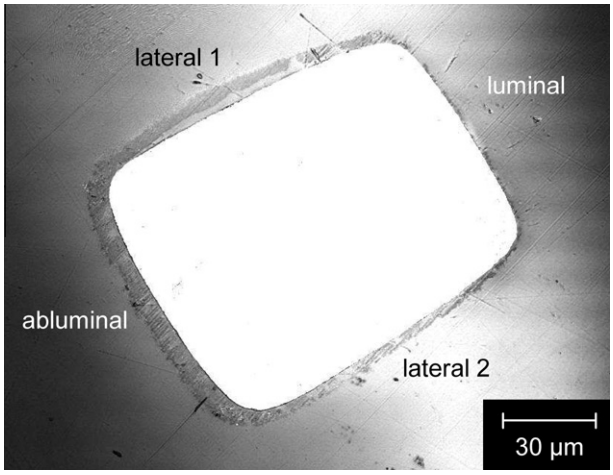

Fig. 13. Representative confocal microscopic image of a polished microsection of a single coated stent strut with the metal core of the stent strut appearing white and the coating appearing grey in this image; location of the different strut sides as indicated.

Table 2
Coating thickness data of the different strut sides of a fluorescein sodium and a triamterene coated stent, $n = 1$ microsection per stent, >175 individual measurements per strut side, mean values ± standard deviations.

	Stent 1 (fluorescein sodium) (μm)	Stent 2 (triamterene) (μm)
Mean coating thickness abluminal	4.6 ± 2.8	5.4 ± 2.2
Mean coating thickness lateral 1	2.9 ± 2.4	3.3 ± 2.3
Mean coating thickness lateral 2	2.7 ± 2.9	4.2 ± 1.9
Mean coating thickness luminal	2.6 ± 2.2	2.7 ± 1.3

The two methods developed to prepare the hydrogel for microscopic examination were well suitable to analyse spatial distributions within the hydrogel compartment. With the two different setups, analysis of diffusion depth as well as examination of the innermost layer of the simulated vessel, which was in direct contact with the DES, became feasible. The examination of the hydrogel samples yielded redistribution process into the perfusion liquid as well as into other hydrogel regions. In contrast to the results presented by Hwang et al. [7], who observed inhomogeneous distributions after 3 h of incubation, the experiments with alginate films yielded homogeneous distributions independent of the distance from the stent struts after only 5 min of incubation. The images of the film which was incubated for 1 min demonstrate that inhomogeneous distributions can be detected using this setup. However, the diffusion in the hydrogel was evidently so fast that homogeneous distributions resulted in the film within about 5 min. Since the diffusion coefficients in water reported for the two model substances hardly deviate from each other (fluorescein sodium 4.25×10^{-4} mm²/s, rhodamine B 4.27×10^{-4} mm²/s [17]) other factors, such as the different coating polymers or the different properties of the acceptor compartments (explanted artery versus hydrogel), have to be held responsible for the different outcomes of the experiments. In this context, it has to be kept in mind that a hydrogel is a simple model for tissue. It neither includes functional structures such as proteins as specific or unspecific binding partners or transporters nor specific characteristics of diseased vessels which may have a great impact on in vivo distributions [18,19]. Also, the composition of the living arterial wall is not homogenous since it consists of layers of different properties [20]. This multi-layer character was not taken into account in the experimental setup and not in the modelling either, since it was designed to simulate the in vitro experiment. Also, further factors influencing in vivo release such as different strut positioning patterns, thrombus formation and compression of arterial structures [21] were not considered. However, the examination of such complex phenomena is usually not intended in in vitro dissolution testing whose main purpose is the examination of drug release and, in the case of DES, distribution under highly standardised and reproducible conditions. Since the gelling of alginates is a process employing very mild conditions, the incorporation of proteins and living cells is possible and might be used to examine the influence of such structures in specialised future experiments. The adaptation of the acceptor compartment in order to mimic the physiological partition coefficient and water content might also be suitable to further improve the predictability of the test method.

The release from DES coated with insoluble or hardly soluble polymers, in which the drugs are dissolved or suspended, occurs mainly by diffusion of the drug substance through the polymer [1,22]. Therefore, release was modelled as a diffusion process in this work, and data are presented over the square root of time. Convective forces which may be dominant in the blood opposed to the predominance of diffusive transport in the vessel wall [21] were not taken into account. The mathematics of mass transfer by diffusion is similar to that of heat conduction problems [23]. This analogy can be used for analytical calculations [24] and also for FE modelling [25]. FE approaches have successfully been employed to analyse diffusive release processes from medicinal products [26] and have been utilised to examine release from DES [27,25], as well. Complex mathematical models have been developed in order to simulate the in vivo release most accurately, accounting for factors such as drug metabolism in the wall [28], tissue micro- and macrostructure including plaque and the influence of strut geometry and embedding during implantation [29,30]. These aspects were not taken into account in the modelling presented here which was designed to model the in vitro release and distribution in the vessel-simulating flow-through cell.

The comparison of diffusive release from an infinite plane sheet and stent coatings of differing thicknesses into infinite stirred media showed that FE simulations can be replaced by analytical calculations if the coating layers are thin compared to the strut edge

length so that the curvature of the coating is negligible. As a further prerequisite, the coatings must be of homogeneous thickness, the release has to be diffusion controlled and the hydrodynamic conditions must be describable by the boundary condition $c = 0$. If these conditions are not fulfilled or more complex geometries (such as geometry 2, 3a and 3b) are to be analysed other methods such as FE methods have to be employed.

The analytical expression (Eq. (2)) was used to calculate the release for coating layer thicknesses of 2 μm using different diffusion coefficients. Based on the comparison of this data to experimental determinations, the diffusion coefficients in the coating were fitted. In the case of triamterene, experimental release from the coating was slower than expected at early time points. This divergence was possibly caused by boundary layer effects which could not be modelled adequately. Because the saturation solubility in the coating material was not determined we assumed a value that equals the amount of drug incorporated in the polymer. An even higher drug solubility should not affect the obtained results very much because of the low volume of the coating compared the hydrogel volume. However, if the actual solubility of the model substance in the coating is lower than assumed in our calculation, a fraction of undissolved drug particles can occur in the coating yield additional inhomogeneities and interfaces. The employed diffusion coefficients were however determined experimentally and therefore represent effective diffusion coefficients which include other effects on the release rate such as the dissolution rate of potentially suspended drug particles. At this point it also has to be noticed that release from the stent coatings presented here was fast compared to what is expected from a clinically applied stent. This may have been caused by the choice of materials (physico-chemical properties of the coating polymer and the model substances) as well as the obtained coating thicknesses which were smaller than those reported for the Cypher® (12,5 μm [31] containing a 5 μm drug storing layer [32]) and the Taxus® (16 μm [31]) stent. However, markedly faster release rates (~70% in 10 h) have also been reported for the Cypher® stent when tested in vitro in the compendial flow-through cell [33] compared to the expected in vivo release of approximately 80% within 30 days [32]. This data suggest that drug release from stents may be considerably faster in large volume in vitro setups.

The diffusion in the hydrogel was modelled via the FE approach since prior comparison of release from a hollow cylinder to a plane sheet of the same thickness yielded distinct differences (data not shown). Mass transport in hydrogels is usually described by diffusion. Deviations from the expected release behaviour are, however, possible in dependency of the dissolution rate in the case of suspended drug, gel erosion, swelling and shrinkage of the gel [34,35] and on the pore size in relation to the size of the transported molecule [36]. Since the alginate hydrogel consisted of approximately 96% water, the solubility of the model substances in the gel was assumed to equal their solubility in water. The determined diffusion coefficient was $D_h = 5 \times 10^{-4}$ mm^2/s for both model substances. This is not surprising, since both substances are relatively small molecules that were fully dissolved in the gel, and electrostatic interactions with the hydrogel backbone were not expected. For fluorescein sodium diffusion coefficients of 4.25×10^{-4} mm^2/s in water [17] and 1-4 $\times 10^{-4}$ mm^2/s in calcium alginate [37] have been reported which are in good accordance with the experimentally determined value.

The comparison of FE and experimental data employing geometry 3a (DES implanted into hydrogel, no perfusion liquid present) also implies that the fitted diffusion coefficients for the stent coating as well as the hydrogel are well suitable to describe the transport processes. The fact that in the case of fluorescein sodium the slowly released fraction of drug was smaller experimentally than modelled indicates that the coating on the luminal side may have been thinner.

The FE modelling of the full three compartment system (geometry 3b) yielded a good general description of the release and distribution behaviour. However, the experimentally determined release occurred slower than expected from the modelled data and the drug fractions in the hydrogel were higher. A comparison of the peak drug fractions determined experimentally in the hydrogel to results obtained via mathematical modelling by other groups also yields comparable results. Pontrelli et al. [24] report on a peak drug concentration of approximately 35% in the arterial wall using diffusion coefficients of heparin as a comparably hydrophilic drug. Mongrain et al. [30] examined the effect of different diffusion coefficients in the polymer and the vessel wall expected for hydrophobic and hydrophilic drugs. The determined concentrations (percentage) in the vessel wall ranged from 1.66% to 30.66% after 1 day using diffusion coefficients ranging from 1×10^{-6} mm^2/s to 1×10^{-8} mm^2/s. With the vessel-simulating flow-through cell, peak concentrations amounted to 27% in the case of fluorescein sodium and 10% for triamterene, respectively. However, the FE modelling presented in this work did not result in the same peak concentrations in the simulated vessel wall.

Two main parameters may be responsible for the discrepancies between the results of the experiments and the FE modelling: the modelling of the perfusion liquid by a boundary condition and the modelling of the coating as a layer of homogeneous thickness. The perfusion liquid was modelled by the boundary condition $c = 0$ which represents infinite perfusion liquid. In the experiments, the amount of perfusion liquid was 250 ml. Due to the volume ratio between perfusion liquid (250 ml) and hydrogel (15 ml), the hydrogel fraction was however only slightly changed by modelling the finite perfusion liquid volume (data not shown). Due to the modelling of infinite perfusion liquid, an equilibrium distribution of the released substance between the hydrogel and the perfusion liquid at the end of the experiment, as observed experimentally, did not evolve in the FE modelling. Furthermore, the partition coefficient was assumed to equal unity for the modelling, which may not represent the situation in the experimental setup accurately. Another drawback of modelling the perfusion liquid via boundary conditions is that hydrodynamic details are not taken into account. The influence of such details has been explored using computational fluid dynamic modelling tools [38,39]. According to the authors, recirculation zones may form close to not fully embedded struts and influence the tissue uptake of drug dissolved in these regions. These results show that in spite of the high flow rates, relatively unstirred diffusion zones separated from the free-flowing perfusion liquid may form which can also possibly influence the release rate from the coating as well as the rate of diffusive washout from the hydrogel into the perfusion liquid.

In an attempt to further improve the fitment of the modelling and to gain an insight into the influence of inhomogeneous coating thicknesses, two cases of asymmetric coating were modelled. The results of the FE modelling show that the abluminally located coatings decelerated the release as intended. Inhomogeneous localisations of coatings in which the coating on the abluminal side is typically much thicker than on the luminal side have been reported in literature [40,41]. Images of scanning electron micrograph cross-sections of the Cypher® and the Taxus® Express and Taxus® Liberté stent showing asymmetric distributions of the coating on the different sides of the stent struts of these commercially available stents have also been published [42,43]. Exemplary measurements of the coating thickness of stents coated by our group yielded asymmetric coatings in which the mean coating thickness was higher on the abluminal side compared to the luminal and lateral sides. However, the difference of coating thickness between the distinct sides was not as pronounced as assumed for the modelling. Accordingly, asymmetric coatings are only partially responsible for the discrepancy between modelled and experimental. Regarding

the coating thickness data, it has to be kept in mind that only one cross-section was analysed per stent and that fairly large coating thickness variations existed within the individual sides which resulted in high standard deviations. Our modelling data suggest that such variations will also influence the release rate. Furthermore, the applied two-dimensional FE model with evenly spaced struts does neither account for the upper and lower edge of the stent nor for inconsistent strut arrangements caused for example by connector hinges which are also likely to influence release and distribution.

5. Conclusion

In this work, different preparation techniques were developed to examine the spatial distribution within the hydrogel compartment of the vessel-simulating flow-through cell in cross-sections as well as along the innermost layer lining the lumen. The initially high concentration gradients in the hydrogel were decreased during further perfusion due to redistribution within the gel and diffusive washout into the perfusion liquid. Homogeneous distributions independent of the distance from the releasing strut were detected within the innermost hydrogel layer lining the lumen after only 5 min. Furthermore, the release and distribution examined in the in vitro experiments were modelled mathematically using FE methods. Mathematical modelling proved a powerful tool in addition to dissolution testing and was used to gain further insight into the experimental results. The comparison of the results of FE modelling employing the experimentally determined diffusion coefficients yielded a reasonable agreement with experimental data. The modelling indicated that inhomogeneous distributions of the coatings around the struts may have influenced the release behaviour. Subsequent analysis of coating thickness distribution yielded higher mean coating thicknesses on the abluminal side compared to the luminal and lateral sides.

Taken together, the vessel-simulating flow-through cell in combination with FE modelling represents a feasible approach for the examination of in vitro release from DES and distribution within a vessel-simulating compartment with particular opportunities regarding the examination of spatial distributions.

Acknowledgements

The authors would like to thank A. Wolter and H. Reiter of the Institute of Pathology, University of Greifswald, for help regarding the preparation of cryosections. Furthermore, we are indebted to I. Rühl, Institute for Biomedical Engineering, University of Rostock, for preparing and polishing cross-sections of the stents.

This project was funded by the European Regional Development Fund (ERDF) and the European Social Fund (ESF) within the collaborative research between economy and science of the state Mecklenburg-Vorpommern and the Federal Ministry of Education and Research (BMBF) within REMEDIS "Höhere Lebensqualität durch neuartige Mikroimplantate" (FKZ: 03IS2081).

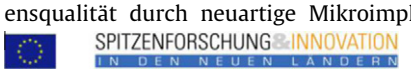

References

[1] S. Venkatraman, F. Boey, Release profiles in drug-eluting stents: issues and uncertainties, J. Control. Release 120 (2007) 149–160.
[2] A.J. Lansky, R.A. Costa, G.S. Mintz, Y. Tsuchiya, M. Midei, D.A. Cox, C. O'Shaughnessy, R.A. Applegate, L.A. Cannon, M. Mooney, A. Farah, M.A. Tannenbaum, S. Yakubov, D.J. Kereiakes, S.C. Wong, B. Kaplan, E. Cristea, G.W. Stone, M.B. Leon, W.D. Knopf, W.W. O'Neill, Non-polymer-based paclitaxel-coated coronary stents for the treatment of patients with de novo coronary lesions: angiographic follow-up of the DELIVER clinical trial, Circulation 109 (2004) 1948–1954.
[3] P.W. Serruys, G. Sianos, A. Abizaid, J. Aoki, P. den Heijer, H. Bonnier, P. Smits, D. McClean, S. Verheye, J. Belardi, J. Condado, M. Pieper, L. Gambone, M. Bressers, J. Symons, E. Sousa, F. Litvack, The effect of variable dose and release kinetics on neointimal hyperplasia using a novel paclitaxel-eluting stent platform: the Paclitaxel In-Stent Controlled Elution Study (PISCES), J. Am. Colloid. Cardiol. 46 (2005) 253–260.
[4] B. Scheller, C. Hehrlein, W. Bocksch, W. Rutsch, D. Haghi, U. Dietz, M. Bohm, U. Speck, Treatment of coronary in-stent restenosis with a paclitaxel-coated balloon catheter, New Engl. J. Med. 355 (2006) 2113–2124.
[5] K.R. Kamath, J.J. Barry, K.M. Miller, The Taxus drug-eluting stent: a new paradigm in controlled drug delivery, Adv. Drug Deliv. Rev. 58 (2006) 412–436.
[6] A.J. Carter, M. Aggarwal, G.A. Kopia, F. Tio, P.S. Tsao, R. Kolata, A.C. Yeung, G. Llanos, J. Dooley, R. Falotico, Long-term effects of polymer-based, slow-release, sirolimus-eluting stents in a porcine coronary model, Cardiovasc. Res. 63 (2004) 617–624.
[7] C.W. Hwang, D. Wu, E.R. Edelman, Physiological transport forces govern drug distribution for stent-based delivery, Circulation 104 (2001) 600–605.
[8] J. Parker, V. Gray, Highlights of the AAPS workshop on dissolution testing for the 21st century, Dissolution Tech. 13 (2006) 26–31.
[9] A. Neubert, K. Sternberg, S. Nagel, C. Harder, K.P. Schmitz, H.K. Kroemer, W. Weitschies, Development of a vessel-simulating flow-through cell method for the in vitro evaluation of release and distribution from drug-eluting stents, J. Control. Release 130 (2008) 2–8.
[10] Council of Europe, European Pharmacopoeia Edition 4.0, 5.0, 6.0 and Supplements, Strassbourg, 2001–2008.
[11] M. Sakai, T. Imai, H. Ohtake, H. Azuma, M. Otagiri, Effects of absorption enhancers on the transport of model compounds in Caco-2 cell monolayers: assessment by confocal laser scanning microscopy, J. Pharm. Sci. 86 (1997) 779–785.
[12] E. Watanabe, M. Takahashi, M. Hayashi, A possibility to predict the absorbability of poorly water-soluble drugs in humans based on rat intestinal permeability assessed by an in vitro chamber method, Eur. J. Pharm. Biopharm. 58 (2004) 659–665.
[13] Y. Zhao, J. Jona, D.T. Chow, H. Rong, D. Semin, X. Xia, R. Zanon, C. Spancake, E. Maliski, High-throughput log P measurement using parallel liquid chromatography/ultraviolet/mass spectrometry and sample-pooling, Rapid Commun. Mass. Spectrom. 16 (2002) 1548–1555.
[14] E. Toropainen, V.P. Ranta, A. Talvitie, P. Suhonen, A. Urtti, Culture model of human corneal epithelium for prediction of ocular drug absorption, Invest. Ophthalmol. Vis. Sci. 42 (2001) 2942–2948.
[15] C. Di Mario, N. Meneveau, R. Gil, P. de Jaegere, P.J. de Feyter, C.J. Slager, J.R. Roelandt, P.W. Serruys, Maximal blood flow velocity in severe coronary stenoses measured with a Doppler guidewire. Limitations for the application of the continuity equation in the assessment of stenosis severity, Am. J. Cardiol. 71 (1993) 54D–61D.
[16] J. Crank, The Mathematics of Diffusion, second ed., Clarendon Press, Oxford, 1998.
[17] C.T. Culbertson, S.C. Jacobson, J.M. Ramsey, Diffusion coefficient measurements in microfluidic devices, Talanta 56 (2002) 365–373.
[18] A.D. Levin, N. Vukmirovic, C.W. Hwang, E.R. Edelman, Specific binding to intracellular proteins determines arterial transport properties for rapamycin and paclitaxel, Proc. Natl. Acad. Sci. USA 101 (2004) 9463–9467.
[19] A.R. Tzafriri, N. Vukmirovic, V.B. Kolachalama, I. Astafieva, E.R. Edelman, Lesion complexity determines arterial drug distribution after local drug delivery, J. Control. Release 142 (2010) 332–338.
[20] G. Pontrelli, F. de Monte, A multi-layer porous wall model for coronary drug-eluting stents, Int. J. Heat Mass Transfer 53 (2010) 3629–3637.
[21] B.M. O'Connell, T.M. McGloughlin, M.T. Walsh, Factors that affect mass transport from drug eluting stents into the artery wall, Biomed. Eng. Online 9 (2010) 15.
[22] F. Alexis, S. Kumar Rath, F. Boey, S. Venkatraman, Study of the initial stages of drug release from a degradable matrix of poly(d,l-lactide-co-glycolide), Biomaterials 25 (2004) 813–821.
[23] H.D. Baehr, K. Stephan, Heat and mass transfer, Springer, Berlin, 1998.
[24] G. Pontrelli, F. de Monte, Mass diffusion through two-layer porous media: an application to the drug-eluting stent, Int. J. Heat Mass Tranfer 50 (2007) 3658–3669.
[25] D.R. Hose, A.J. Narracott, B. Griffiths, S. Mahmood, J. Gunn, D. Sweeney, P.V. Lawford, A thermal analogy for modelling drug elution from cardiovascular stents, Comput. Methods Biomech. Biomed. Eng. 7 (2004) 257–264.
[26] Y. Zhou, X.Y. Wu, Finite element analysis of diffusional drug release from complex matrix systems. I. Complex geometries and composite structures, J. Control. Release 49 (1997) 277–288.
[27] R. Mongrain, R. Leask, J. Brunette, I. Faik, N. Bulman-Feleming, T. Nguyen, Numerical modeling of coronary drug eluting stents, Stud. Health Technol. Inform. 113 (2005) 443–458.
[28] G. Pontrelli, F. de Monte, Modeling of mass dynamics in arterial drug-eluting stents, J. Porous Media 12 (2009) 19–28.
[29] G. Vairo, M. Cioffi, R. Cottone, G. Dubini, F. Migliavacca, Drug release from coronary eluting stents: a multidomain approach, J. Biomech. 43 (2010) 1580–1589.
[30] R. Mongrain, I. Faik, R.L. Leask, J. Rodes-Cabau, E. Larose, O.F. Bertrand, Effects of diffusion coefficients and struts apposition using numerical simulations for drug eluting coronary stents, J. Biomech. Eng. 129 (2007) 733–742.
[31] C.G. Hopkins, P.E. McHugh, J.P. McGarry, Computational investigation of the delamination of polymer coatings during stent deployment, Ann. Biomed. Eng. 38 (2010) 2263–2273.

[32] M.C. Morice, P.W. Serruys, J.E. Sousa, J. Fajadet, E. Ban Hayashi, M. Perin, A. Colombo, G. Schuler, P. Barragan, G. Guagliumi, F. Molnar, R. Falotico, A randomized comparison of a sirolimus-eluting stent with a standard stent for coronary revascularization, New Engl. J. Med. 346 (2002) 1773–1780.
[33] R. Jabara, N. Chronos, K. Robinson, Novel bioabsorbable salicylate-based polymer as a drug-eluting stent coating, Catheter. Cardiovasc. Interv. 72 (2008) 186–194.
[34] A.H. Muhr, J.M.V. Blanshard, Diffusion in gels, Polymer 23 (1982) 1012–1026.
[35] I. Colombo, M. Grassi, R. Lapasin, S. Pricl, Determination of the drug diffusion coefficient in swollen hydrogel polymeric matrices by means of the inverse sectioning method, J. Control. Release 47 (1997) 305–314.
[36] E. Pasut, R. Toffanin, D. Voinovich, C. Pedersini, E. Murano, M. Grassi, Mechanical and diffusive properties of homogeneous alginate gels in form of particles and cylinders, J. Biomed. Mater. Res. A 87 (2008) 808–818.
[37] Ø. Holte, H.H. Tønnesen, J. Karlsen, Effect of charge and size of diffusing probe on the diffusion through calcium alginate gel matrices, Pharmazie 62 (2007) 914–918.
[38] B. Balakrishnan, A.R. Tzafriri, P. Seifert, A. Groothuis, C. Rogers, E.R. Edelman, Strut position, blood flow, and drug deposition: implications for single and overlapping drug-eluting stents, Circulation 111 (2005) 2958–2965.
[39] V.B. Kolachalama, A.R. Tzafriri, D.Y. Arifin, E.R. Edelman, Luminal flow patterns dictate arterial drug deposition in stent-based delivery, J. Control. Release 133 (2009) 24–30.
[40] K. Sternberg, S. Kramer, C. Nischan, N. Grabow, T. Langer, G. Hennighausen, K.P. Schmitz, In vitro study of drug-eluting stent coatings based on poly(L-lactide) incorporating cyclosporine A – drug release, polymer degradation and mechanical integrity, J. Mater. Sci. Mater. Med. 18 (2007) 1423–1432.
[41] A. Belu, C. Mahoney, K. Wormuth, Chemical imaging of drug eluting coatings: combining surface analysis and confocal Raman microscopy, J. Control. Release 126 (2008) 111–121.
[42] L.E. L Perkins, K.H. Boeke-Purkis, Q. Wang, S.K. Stringer, L.A. Coleman, XIENCE V everolimus-eluting coronary stent system: a preclinical assessment, J. Interv. Cardiol. 22 (2009) 28–40.
[43] J. Doostzadeh, L.N. Clark, S. Bezenek, W. Pierson, P.R. Sood, K. Sudhir, Recent progress in percutaneous coronary intervention: evolution of the drug-eluting stents, focus on the XIENCE V drug-eluting stent, Coron. Artery Dis. 21 (2010) 46–56.